

Experimental Evaluation of Game Theoretic Power Allocation in MIMO Ad-hoc Networks

Nicholas J. Kirsch, *Student Member, IEEE*, John Kountouriotis, *Student Member, IEEE*,
Chao Liang, *Student Member, IEEE*, and Kapil R. Dandekar, *Senior Member, IEEE*

Abstract—Multiple input multiple output (MIMO) communication systems in an ad-hoc network can provide high spectral efficiency. Several resource allocation methods have been presented and experimentally demonstrated to improve performance in a resource limited environment. Recently, a game theoretic method has been published with promising results. The goal of this paper is to present simulation and experimental results for this game theoretic technique.

Index Terms—MIMO systems, game theory, local area networks, co-channel interference.

I. INTRODUCTION

MULTIPLE input multiple output (MIMO) systems have proven to be very promising for increasing spectral efficiency of ad-hoc networks [1]. Efficient use of frequency and power is an important goal of any resource limited system. Recent work has shown that these systems can have increased capacity through improved power control. Power control, or resource allocation, is accomplished by assigning power to eigenmodes of the MIMO matrix channel that provide the best capacity. In an interference free system, the optimal solution is independent waterfilling (IWF)[2].

At the expense of network overhead and computational complexity, sophisticated power allocation methods can be used to increase system capacity by limiting external interference, such as multi-user waterfilling (MUWF) and the global gradient projection method (GGP) [3]. MUWF improves capacity by channel whitening. The GGP method improves capacity by globally calculating power to determine the best power allocation. Recent work has been published that takes a game theoretic (GT) approach to the resource allocation problem. This iterative, distributed technique has been shown to outperform MUWF and approach the performance of GGP using energy efficiency and capacity as a metric [4]. While experimental characterization has been performed on the MUWF and GGP techniques [5], the purpose of this letter is to show experimental results for the GT method and compare them with simulations in a similar environment.

In the following section, the system model will be described along with details on the MUWF and GGP power allocation

Manuscript received June 30, 2008; revised November 19, 2008; accepted January 20, 2009. The associate editor coordinating the review of this letter and approving it for publication was E. Hossain.

This research is supported by the National Science Foundation under Grant 0322795, 0322797, and 0435401. National Instruments has provided equipment donations supporting this research.

The authors are with the Department of Electrical and Computer Engineering, Drexel University, Philadelphia, PA 19104-2875 (e-mail: (njk27, jk368, c198, dandekar)@drexel.edu).

Digital Object Identifier 10.1109/TWC.2009.080863

methods. In Section III, the GT method is reviewed. A description of the simulations, measurements, and experimental topology are provided in Section IV. Finally, Section V includes the results.

II. FORMULATION

The network of interest consists of $\mathcal{L} = \{1, 2, \dots, L\}$ links and each link receives interference from the other links, with N_r receive antennas and N_t transmit antennas. For a particular link, l , the received signal is $y_l = \mathbf{H}_{l,l}\mathbf{x}_l + \sum_{j=1, j \neq l}^L \mathbf{H}_{l,j}\mathbf{x}_j + \mathbf{n}_l$, where $\mathbf{H}_{l,l}$ is an $N_r \times N_t$ channel matrix, \mathbf{x}_l is the transmitted signal, and \mathbf{n}_l is the Gaussian background noise. The two subscripts of the channel matrix refer to the receiver and transmitter of a particular link.

The capacity for a link of interest l is calculated with,

$$C_l(\mathbf{Q}_1, \dots, \mathbf{Q}_L) = \log_2 \det(\mathbf{I} + \mathbf{H}_{l,l}\mathbf{Q}_l\mathbf{H}_{l,l}^\dagger\mathbf{R}_l^{-1}) \quad (1)$$

where the power allocation matrix for link l is $\mathbf{Q}_l = E\{\mathbf{x}_l\mathbf{x}_l^\dagger\}$ and $\mathbf{R}_l = \mathbf{I} + \sum_{j=1, j \neq l}^L \mathbf{H}_{l,j}\mathbf{Q}_j\mathbf{H}_{l,j}^\dagger$ is the covariance matrix of the interference-plus-noise. \mathbf{R}_l is a function of the sum of interfering links. The sum-rate capacity can be determined by

$$C(\mathbf{Q}_1, \dots, \mathbf{Q}_L) = \sum_{l=1}^L C_l \quad (2)$$

The capacity for a given network will vary depending on the method that each link calculates each \mathbf{Q}_l . For our analysis, we are leaving out IWF and focusing on power allocation methods that consider co-channel interference.

MUWF increases capacity by taking into consideration the interfering channels. Therefore, the channel of the link of interest $\mathbf{H}_{l,l}$ is whitened with the interference-plus-noise covariance matrix, \mathbf{R}_l . For the MUWF power allocation method, the channel for the link of interest in Eq. 1 is, $\tilde{\mathbf{H}}_{l,l} = \mathbf{R}_l^{-1/2}\mathbf{H}_{l,l}$. This distributed approach improves capacity over IWF in an interference limited system at the cost of more complexity, i.e. the knowledge of interfering links included in \mathbf{R}_l .

A centralized approach is the GGP method, which assumes complete channel knowledge to perform a globally optimal power allocation. This method provides higher system capacity, but is not distributed. GGP power allocation is based on the steepest descent method which maximizes the sum capacity over all links,

$$\max_{\mathbf{C}_l} \sum_{i=1}^L C_i(\mathbf{Q}_1, \dots, \mathbf{Q}_L). \quad (3)$$

This letter describes the experimental performance of game theoretic power allocation in comparison with other methods. Further specifics on MUWF and GGP can be found in [3].

III. GAME THEORY

The game theory power allocation method is a distributed system where each “player” or link controls its power based upon the utility (i.e. capacity) of a link and a penalty function for transmitting power. The utility of a link is the link capacity, C_l , which is a function of the squared singular value of the whitened channel, $\sigma_{l,i}$. The penalty or pricing function is then a function of the amount of power a link uses, p_l , to prevent a link from transmitting unnecessarily high power. p_l is scaled by a pricing factor γ_l to enforce a minimum capacity per unit power. Therefore, the net-utility function can be expressed as, $u_l = C_l - \gamma_l p_l$. With this net-utility function, the per-link objective function can be expressed as,

$$\max_{\mathbf{z}_l} \sum_{i=1}^{N_t} \log_2(1 + z_{l,i} \sigma_{l,i}) - \gamma_l \sum_{i=1}^{N_t} z_{l,i} \quad (4)$$

such that $\sum_{i=1}^{N_t} z_{l,i} \leq p_l$, which is the total power constraint. Further, the value of γ_l must be selected. Details for computing γ_l are described in [4] along with the complete details of how links can be shutdown completely if their capacity does not exceed a pre-specified threshold. In this paper, a “soft shutdown” mechanism is used for γ_l . This mechanism sets γ_l such that most links use less than maximum power.

Quantitatively, the MUWF and GT methods are similar in that they both maximize the capacity of each user, which means that the power covariance matrix for each user is of the form $\mathbf{Q}_l = \mathbf{V}_w \mathbf{Z} \mathbf{V}_w^H$, where \mathbf{V}_w comes from the SVD of the *whitened channel matrix*, $\mathbf{H}_w = \mathbf{R}^{-1/2} \mathbf{H} = \mathbf{U}_w \mathbf{\Sigma} \mathbf{V}_w^H$. Notice that the whitened channel matrix per user can be different for MUWF and GT, since some links are shutdown and transmitted power per link is different even though they start with the same total available power.

In the GGP method, the objective is no longer to maximize the capacity of each user, but rather to maximize the sum capacity of the network. Therefore, the eigenvectors of \mathbf{Q}_l no longer coincide with the right unitary matrix of the SVD of the whitened channel matrix. This occurs because the choice of optimal \mathbf{Q}_l per user is affected, not only by the resulting single user capacity, but also by interference imposed to others via the interference plus covariance matrix (\mathbf{R}_l). Thus, the eigenvectors that find a “sweet spot” between the two objectives (single user capacity and interference imposed on other users) are used. These eigenvectors are usually different from the eigenvectors of the whitened channel matrix.

IV. SIMULATIONS AND MEASUREMENTS

A. Simulation Information

To simulate an indoor environment to determine the performance of the different power allocation methods, the ray tracing program FASANT [6], [7] was used with a 3-D model of the Bossone environment. The 3-D indoor model includes all major walls and floors using relative permittivity and permeability for those objects: $\epsilon_r = 4.44$, $\mu_r = 0.99$

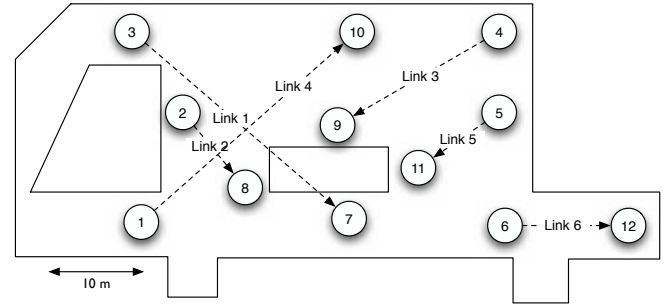


Fig. 1. Nodes locations and one topology used for measurements and simulations in the Bossone building.

and $\epsilon_r = 3$, $\mu_r = 0.99$ respectively. Only major features were included and no additional scattering bodies were in the simulation environment. Simulations were run at a frequency of 2.484 GHz at the same locations as in the measurements. The antenna arrays were modeled as dipoles in the simulation package FEKO [8], due to the unavailability of precise radiation patterns of our antennas. Radiation patterns for these near field simulations were used as an input to FASANT. We have previously used this simulation scheme to simulate MIMO network links [4], [5]. At each location, simulations were performed in a 10×10 grid of positions with separation $\lambda/10$. The channel response from this grid of positions were used to provide local averaging to reduce the effects of small scale fading.

B. Experimental Testbed

The channel measurements for this letter were performed with a custom software defined radio multiple antenna system. The nodes were created at the Drexel University Wireless Systems Laboratory in collaboration with the University of Texas - Austin Wireless Networking & Communications Group. The measurements for determining the channel gains were made with a carrier frequency of 2.484 GHz, on a BPSK signal with 5 MHz bandwidth. The baseband processing is based upon the 802.11g standard in SDM mode. Specifically, the preamble of the standard (channel training) was used for capturing the channel. For this MIMO network, two omni-directional MAXRAD 6 dBi antennas were used at each node, with an inter-element spacing of $\lambda/2$.

The measurements were made on the third floor of the Bossone building at Drexel University. The node locations ($\text{Tx}:\{1, \dots, 6\}$ and $\text{Rx}:\{7, \dots, 12\}$) are shown in Fig. 1. The antenna arrays are all oriented vertically with respect to the figure. We used two nodes (one transmitter and one receiver) to create a simulated multi-node topology. By changing the location of these two nodes, many different topologies can be constructed. The two nodes were positioned at each Tx and Rx position where 100 channel snapshots were measured. For example, the channel from $\text{Tx}:1$ to $\text{Rx}:7$ was measured and then the channel from $\text{Tx}:1$ to $\text{Rx}:8$ was measured. First, the links are used to measure a single topology shown with lines from the transmitter to an arrow denoting the receiver as in Fig. 1. Second, from all of the Tx and Rx positions, 720 six-node topologies are considered in the multi-topology analysis.

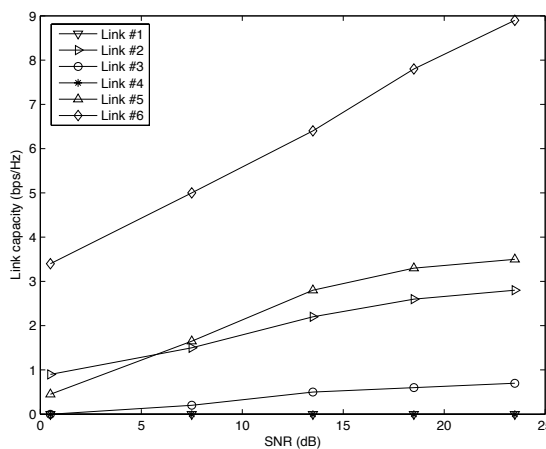


Fig. 2. Measured link capacity versus SNR with GT power allocation in the topology shown in Fig. 1.

Therefore, we present the performance of the different power allocation methods for a single topology of interest and every possible six node topology.

During the channel measurement, we tried to keep the environment as stable as possible by limiting people from walking by and opening doors. After the channels were recorded, the three different power allocation methods were used to calculate the capacity off-line. The total power available for each link was initialized to 20 dB. For each topology, the instantaneous capacity was calculated for the 100 snapshots. In a real-time wireless communication system, once all the channels were determined at the receiver of a particular link, the channels would be sent to the transmitter which would then calculate power allocation.

V. RESULTS

The first set of results is presented in Fig. 2, which shows the measured link capacity for one topology of interest (out of the 720 possible six-node topologies), using GT, for increasing values of SNR. From the chosen topology (Fig. 1), one can see how these capacities are achieved. First, because link 6 is more isolated than the other links, the receiver is less affected by other transmitters. Next, the transmitter of link 6 has little effect on the other receivers. Therefore, more capacity can be achieved by the channel that has little interference. Third, both links 1 and 4 are susceptible to greater sources of interference and would not yield much capacity without greater signal power. Therefore, these links are shut-down to prevent unnecessary interference to the rest of network. Links 5 and 2 are similar to each other and are moderately affected by interfering links because the receivers of these links are in a centralized location. Finally, link 3 is able to achieve a relatively small level of capacity amidst the co-channel interference.

Table I is the comparison of the measured sum-rate capacity and the efficiency results from this topology using different power allocation schemes. The energy efficiency λ , is the ratio of the network capacity to the total network power (bps/Hz/W). With 20 dB of SNR, GT has a sum-rate capacity

TABLE I
MEASURED SUM-RATE CAPACITY AND EFFICIENCY FOR SINGLE TOPOLOGY
WITH SNR=20 dB

Allocation scheme	Capacity (bps/Hz)	Efficiency
MUWF	11.56	0.0193
GGP	16.52	0.0275
GT	13.22	0.0314

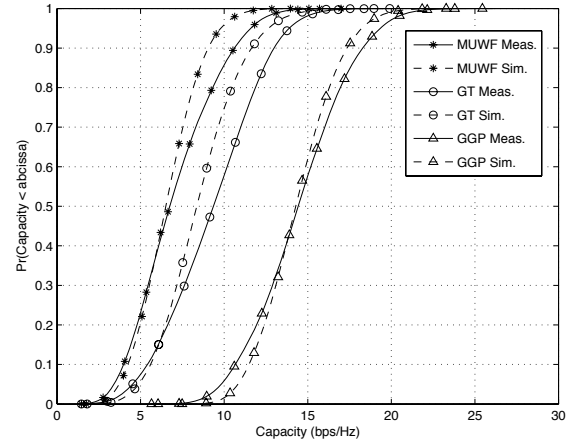


Fig. 3. CDF of sum-rate capacities for different methods from measurements and simulations over all topologies.

between MUWF and GGP. However, this specific topology is an example of the GT method providing higher efficiency than the GGP method. This condition occurs due to the GT method using lower transmit powers. These results match the interpretation that GT is an improvement over MUWF. The GGP method is able to achieve greater capacity due to its use of greater levels of network information (and overhead).

Next, with 720 six-link topologies and data from 100 locations and snapshots from simulations and measurements respectively, the sum-rate capacity was calculated and the cumulative distribution function (CDF) for the three resource allocation schemes is shown in Fig. 3. The capacity for GT is higher than the MUWF case, however not as high as the GGP method. The GGP method assumes a centralized control with complete channel knowledge of all links, which allows for an optimal solution to be found. The GT approach utilizes penalties for using too much power over weak channels, thus the capacity results are greater than the MUWF scheme. The measurements results are fairly similar to the simulations for all of the power allocation schemes. Differences can be attributed to the fact that the simulations can not possibly reproduce all of the channel effects in a real environment, notably scattering. Also, the measurement locations may not be precisely in the same location as in the simulation environment.

Further, we show the CDF of the energy efficiency, Fig. 4 for simulated and measured topologies. These results show that for all topologies, the GT method is more energy efficient than MUWF method and nearly as efficient as the GGP method. There are some cases when the GT method is actually more efficient than the GGP method. While the capacity

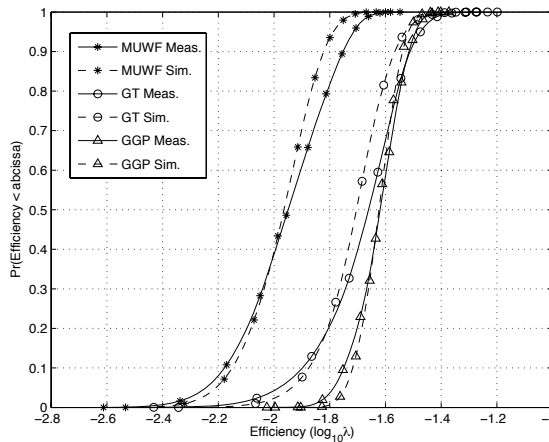


Fig. 4. CDF of energy efficiencies for different methods from measurements and simulations over all topologies.

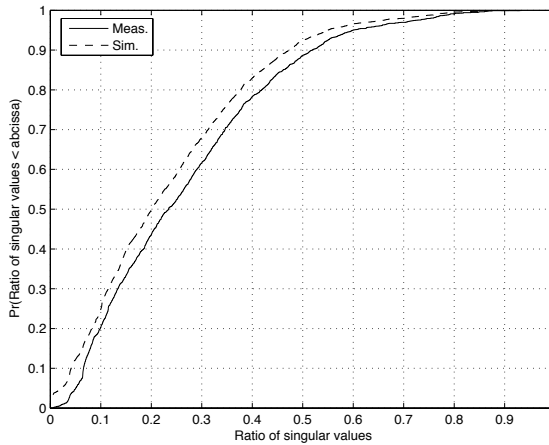


Fig. 5. CDF of the ratio of singular values from measurements and simulations.

performance of the GT method was near MUWF, the energy efficiency is closer to GGP. This is due to the soft-shutdown mechanism, which limits the transmitted power of links with little achievable capacity. As with the capacity CDF results, energy efficiency CDF results show good agreement between measurements and simulations.

To provide a comparison between measured and simulated channels, Fig. 5 shows a CDF of the ratio of singular values (smaller singular value over larger singular value) for measured and simulated channels. Fig. 5 shows the distribution of

the singular value ratios for the 3,600 (i.e., 6 transmit positions \times 6 receive positions \times 100 samples) measured and simulated channels. The ratio is greater for the measured channels, which shows that the measured channels are more uncorrelated. This result makes sense because simulated channels are an approximation of the actual environment and do not include all possible features in the multipath environment. These additional multipath features have been shown to decrease channel correlation and increase singular value ratios [9]. It is important to note that the distributions are very similar except that the measured channels are shifted to higher ratios.

VI. CONCLUSION

In this letter, experimental and simulated results for different power allocation methods in an indoor MIMO local area network have been shown. The performance of the GT method was compared to MUWF and GGP methods in terms of capacity and energy efficiency. Additionally, the probabilistic results show that the GT method outperforms the MUWF approach and approaches the performance of the GGP method (without as much network overhead). These results quantify the benefits, in terms of capacity and energy efficiency, of using greater levels of network knowledge in MIMO ad-hoc network power allocation.

REFERENCES

- [1] G. J. Foschini and M. J. Gans, "On the limits of wireless communications in a fading environment when using multiple antennas," *Wireless Personal Commun.*, vol. 6, pp. 331–335, Mar. 1998.
- [2] T. M. Cover and J. A. Thomas, *Elements of Information Theory*. New York: Wiley, 1991.
- [3] S. Ye and R. S. Blum, "Optimized signaling for MIMO interference systems with feedback," *IEEE Trans. Signal Processing*, vol. 51, pp. 2839–2848, Nov. 2003.
- [4] C. Liang and K. R. Dandekar, "Power management in MIMO ad hoc networks: a game-theoretic approach," *IEEE Trans. Wireless Commun.*, vol. 6, no. 4, pp. 2839–2848, Apr. 2007.
- [5] N. J. Kirsch, C. Liang, and K. R. Dandekar, "Experimental characterization of resource allocation algorithms in MIMO-OFDM ad hoc networks," in *Proc. IEEE Radio and Wireless Symposium*, 2007.
- [6] F. S. de Adana, O. Gutierrez, I. G. Diego, J. P. Arriaga, and M. Catedra, "Propagation model based on ray tracing for the design of personal communication systems in indoor environments," *IEEE Trans. Veh. Technol.*, vol. 49, no. 6, pp. 2105–2112, Nov. 2000.
- [7] M. Catedra and J. Perez-Arriaga, *Cell Planning for Wireless Communications*. Boston, MA: Artech House, 1999.
- [8] D. Davidson, I. Theron, U. Jakobus, F. Landstorfer, F. Meyer, J. Mostert, and J. V. Tonder, "Recent progress on the antenna simulation program FEKO," in *Proc. 1998 South African Symposium on Communications and Signal Processing*, vol. 1, Sept. 1998, pp. 427–430.
- [9] M. Ozdemir, E. Arvas, and H. Arslan, "Dynamics of spatial correlation and implications on MIMO systems," *IEEE Commun. Mag.*, vol. 42, no. 6, pp. S14–S19, June 2004.